Breather Transitions and Their Mechanisms of a (2+1)-Dimensional Sine-Gordon Equation and a Modified Boussinesq Equation in Nonlinear Dynamics

Qian Gao[1] · Shou-Fu Tian[1] · Ji-Chuan Liu[1] · Yan-Qiang Wu[1]

Abstract

Studying the transformation mechanisms of soliton solutions of some high-dimensional equations can aid in comprehending the physical phenomena of the relevant nonlinear wave interactions. Therefore, the transitions and mechanisms of nonlinear waves in the (2+1)-dimensional sine-Gordon and (2+1)-dimensional modified Boussinesq equations are investigated for the first time by means of characteristic line and phase shift analysis, and the dynamic behavior of various nonlinear transformed waves is analyzed. Firstly, we derive the N-soliton solution by applying the Hirota bilinear method, from which the breather solution is constructed by changing the parameters into a complex form in pairs. In addition, via the characteristic-line analysis, we present the mechanism for the transformation of the breather solution, which is composed of the nonlinear superposition of a solitary wave and periodic wave. When the characteristic lines of the two parts are parallel, we find that various transformed nonlinear wave structures can be obtained, such as M-type solitons, oscillating M-type solitons, multi-peak solitons, quasi-sine waves and so on. Finally, we demonstrate that the geometric properties of the characteristic lines vary with time essentially resulting in the time-varying properties of nonlinear waves, which have never been found in (1+1)-dimensional systems. Overall, the study of breath-wave transitions in the (2+1)-dimensional sine-Gordon equation and the modified Boussinesq equation provides valuable insights into the bahavior of nonlinear systems and wave propagation.

✉ Shou-Fu Tian
  sftian@cumt.edu.cn; shoufu2006@126.com

✉ Ji-Chuan Liu
  liujichuan2003@126.com

✉ Yan-Qiang Wu
  wyq1976819@cumt.edu.cn

[1] School of Mathematics, China University of Mining and Technology, Xuzhou 221116, People's Republic of China

Birkhäuser

1 Introduction

Soliton theory was developed in the 1840s, and has become an important means to study nonlinear science [1]. Soliton is a quasi-particle that is morphologically stable and excited by a nonlinear field with non-dispersive energy. Soliton possesses all the properties of particles, including energy, momentum, and mass, and so on. They also adhere to all the laws of nature [2, 3]. It can describe some physical phenomena, and is widely used to explain water wave propagation in rivers and oceans, signal transmission in optical fiber communication, and some special phenomena in the field of plasma physics [4–6]. Some eloquent developments in nonlinear physics have been made [7–9]. The discovery of soliton phenomena can be traced back to 1844, when British scientist Scott Russell [10] accidentally discovered a strange phenomenon of water waves while walking in the river. Since then, the concept of soliton waves entered everyone's vision. Subsequently, in 1895, Korteweg and Vries introduced the signature KdV equation for isolated waves [11], and since then, the existence of solitary waves has been widely recognized by the academic community. In 1965, Zabusky and Kruskal used numerical methods to study the interaction process of solitary waves in plasma, and confirmed that the waveforms do not change after the interaction of solitary waves, and were named soliton [12]. The development of soliton is of great significance to mathematics and other scientific fields [13–17]. At present, soliton theory seems to have shown its vigorous vitality, and has become a new science, and its research will undoubtedly promote the development of modern mathematical physics and applied engineering [18–22].

There are many famous methods to derive the soliton solution of the nonlinear equation, such as inverse scattering method [23], Bäckloud transformation method [24], Lie group method [25], Darboux transformation method [26] and Hirota bilinear method [27]. In addition, there are various methods to derive soliton solutions of the nonlinear equation [28]. The Hirota bilinear method applied in this paper is proposed by Hirota in 1971 [29]. It is a powerful tool to construct analytical solutions [30–32]. Moreover, some new works find new properties of PDEs by using bilinear method [33–35]. We apply the bilinear method in this work, which has the advantages of simplicity and directness. It does not require that the nonlinear partial differential equations under study have Lax pairs, i.e., regardless of the existence of Lax pairs in equations, the equations can be solved directly by transforming them into bilinear type by means of bilinear transformations.

In addition, solitons with different structures have also been studied, such as the dark solitons [36], anti-dark solitons [37], W-type solitons [38] as well as multi-solitons [39, 40]. The concept of rogue wave [41] was proposed by the British writer Darp, which is a peak value structure with limitations in space and time, and it is also known as the wave of "coming without shadow, going without trace". Breathers are nonlinear waves that are periodic in both time and space, and can be divided into Akhmediev breathers [42] and Kuznetsov-Ma breathers [43]. Akhmediev breathers are periodic and completely localized in the direction of evolution, while Kuznetsov-Ma breathers are periodic and localized in the direction of evolution. Many mathematical models can describe these nonlinear waves, such as the Korteweg-de Vries (KdV) equation

[11] and the nonlinear Schrödinger (NLS) equation [44], as well as their various deformations.

The breather is a local wave that exhibits periodic oscillation behavior in a certain direction [45]. Recent studies have shown that breather solutions exist for many nonlinear equations, including sine-Gordon equation [46], Kudryashov-Sinelshchikov equation [47], (4+1)-dimensional Fokas equation [48], Korteweg-de Vries (KdV) equation [49]. Lump is derived from breather degradation (period is infinite), that is, a limiting structure of breather [50]. Under certain conditions, breathers and rogue waves can be converted into other types of nonlinear waves, referred as the state transformation of waves [51, 52].

In nonlinear systems, higher-order effects and coupling effects have significant effects on the state transformation of nonlinear waves. In this case, the breather can be seen as a single pulse composed of a nonlinear superposition of a solitary wave component and a periodic wave component with their own velocities V_s and V_p. In general, the velocity difference between the two components is not zero, that is, $V_s \neq V_p$. Conversely, if $V_s = V_p$, the breather can be transformed into other nonlinear waves, such as antidark solitons ($\eta_s \neq 0$, $\eta_p = 0$), M-type or W-type solitons ($\eta_s \approx \eta_p$), multi-peak solitons ($\eta_s < \eta_p$), periodic wave ($\eta_s = 0$, $\eta_p \neq 0$), where η_s, η_p represents the wave number of the solitary wave component and the periodic wave component, respectively. Moreover, in recent years, some rich nonlinear wave structures have been discovered in the plane wave background in the higher-order nonlinear equations. [53] proved that the breathers in the higher-order NLS equation can be converted into non-pulsed solitons. The conservation between rogue waves and W-type solitons in the Hirota equation has been discovered, which is influenced by higher-order effects [54]. Breather-to-soliton transitions, nonlinear wave interactions, and modulational instability have been found in a higher-order generalized nonlinear Schrödinger equation [55]. In addition, the (2+1)-dimensional KdV equation and the state transition between lump wave and breather have been studied in [56].

In view of previous studies, the transformation mechanism for the (2+1)-dimensional sine-Gordon equation and (2+1)-dimensional modified Boussinesq equation has not yet been studied. Motivated by these, we investigate nonlinear wave state transitions for the (2+1)-dimensional sine-Gordon equation [57] and the (2+1)-dimensional modified Boussinesq equation [59].

The (2+1)-dimensional sine-Gordon equation is given as follows:

$$u_{xx} + u_{yy} - u_{tt} = \sin u. \tag{1.1}$$

Equation (1.1) is the classical wave equation with a nonlinear sine source term. The sine-Gordon partial differential equations can be used to simulate the dynamic mechanism of base motion during DNA transcription and remaking. The equations are widely used in research because of their adaptability, nonlinearity and increasing dispersion accuracy. [58] derived localized dynamical behavior in the (2+1)-dimensional sine-Gordon equation. [60] studied new kink-shaped solutions and periodic wave solutions for the (2+1)-dimensional sine-Gordon equation. New class of running-wave solutions of the (2+1)-dimensional sine-Gordon equation have also been given in [61].

Here we take

$$u = 2i \ln \left(\frac{f^*}{f} \right), \tag{1.2}$$

where f is any complex function, $*$ denotes the complex conjugate, and $i = \sqrt{-1}$
Then we get the bilinear form of the (2+1)-dimensional sine-Gordon equation:

$$(D_x^2 + D_y^2 - D_t^2)(f \cdot f) = \frac{1}{2}(f^2 - (f^*)^2), \tag{1.3}$$

where D_x, D_y and D_t are bilinear operators. They are defined by

$$D_t^m D_x^n D_y^p(f \cdot g) = (\partial_t - \partial_{t'})^m (\partial_x - \partial_{x'})^n (\partial_y - \partial_{y'})^p$$
$$[f(t, x, y)g(t', x', y')]|_{t'=t, x'=x, y'=y}. \tag{1.4}$$

The (2+1)-dimensional modified Boussinesq equation is given as follow:

$$u_{tt} - u_{xx} - u_{yy} - 3 \left(u^2 \right)_{xx} - u_{xxxx} = 0. \tag{1.5}$$

The standard Boussinesq equation is often used to describe the propagation and change
of nonlinear shallow water waves, including shallow water deformation, reflection,
diffraction, refraction, wave breaking and dissipation, wave current interaction, and
tidal current phenomenon caused by waves [62, 63]. Solutions and conservation laws
of a (2+1)-dimensional Boussinesq equation have been given [64]. The decomposition
method for solving (2+1)-dimensional Boussinesq equation have also been studied in
[65]. [66] researched on lump solution of (2+1)-dimensional Boussinesq equation.
This paper is evolved from the generalized (2+1)-dimensional Boussinesq equation,
which is shown as follows:

$$u_{tt} + \alpha u_{xx} - u_{yy} + \beta \left(u^2 \right)_{xx} + \gamma u_{xxxx} = 0.$$

When $\alpha = -1, \beta = -3, \gamma = -1$, it is the (2+1)-dimensional modified Boussinesq
equation.

In order to obtain the bilinear form of equation (1.5), first we let

$$u = 2(\ln f)_{xx}. \tag{1.6}$$

Substituting Eq. (1.6) into Eq. (1.5) , we get:

$$(D_t^2 - D_x^2 - D_y^2 - D_x^4)(f \cdot f) = 0. \tag{1.7}$$

The main purpose of this work is to study the state transition of nonlinear waves and
various properties of transformed waves via nonlinear superposition, characteristic
lines and phase shift analysis of the (2+1)-dimensional sine-Gordon equation and the

Table 1 Various types of transformed waves and corresponding wave parameters

Transformed nonlinear waves	Wave parameters (a_1, b_1)
Quasi-anti-dark soliton	$a_1 = 3, b_1 = 1$
M-type soliton	$a_1 = 1, b_1 = 1$
Oscillating M-type soliton	$a_1 = 1, b_1 = 2$
Multi-peak soliton	$a_1 = 1, b_1 = 5$
Quasi-sine wave	$a_1 = 0.001, b_1 = 1$
Quasi-periodic anti-dark soliton	$a_1 = 0.001, b_1 = 3$

(2+1)-dimensional modified Boussinesq equation. Thus, following problems need to be further considered:

- What is the nonlinear superposition mechanism of the breathers of these two equations?
- Do state transition conditions exist for breathers?
- How does time change affect nonlinear waves?

In addition, compared with previous studies, we also have some innovations, which are as follows:

- According to the Hirota method, we derive the breather solutions and some conversion waves of the two equations for the first time.
- We also present a certain nonlinear superposition mechanism of some breathers. The breathers and transformed waves are the nonlinear superpositions of solitary and periodic waves. Those results help us understand some structures of the transformed solutions.
- The characteristic lines of the transformed waves are parallel, and the distance between them is a function of the time t. As the time changes, the geometry of the characteristic lines also changes, thus having the evolution of the other transformed waves. It is helpful for finding various types of solutions with position and range requirements.

1.1 Main Results

Theorem 1.1 *The transformed wave solution $\widetilde{u}_2$ of the breather for the (2+1)-dimensional sine-Gordon equation can be expressed as:*

$$\widetilde{u}_2 = 2i \ln\left(\frac{(2\sqrt{\lambda_2}\cosh(\theta_1 + \ln\sqrt{\lambda_2}) + \lambda_3\cos\Lambda_1)^*}{2\sqrt{\lambda_2}\cosh\theta_1 + \ln\sqrt{\lambda_2} + \lambda_3\cos\Lambda_1}\right), \qquad (1.8)$$

where parameters a_1, b_1 are arbitrary constant, $\theta_1, \lambda_2, \lambda_3, \Lambda$ are defined in Eq. (2.23). The relationship between various types of transformed waves and parameters is shown in Table 1.

Remark 1 The constants a_1, b_1 in Eq. (2.23) control the locality and oscillation of the transformed wave respectively. The larger the value of $a_1(b_1)$, the stronger locality (oscillation) the wave is.

Table 2 Various types of transformed waves and corresponding wave parameters

Transformed nonlinear waves	Wave parameters (a_1, b_1)
Quasi-anti-dark soliton	$a_1 = 2, b_1 = 2$
Oscillating M-type soliton	$a_1 = 1, b_1 = 2$
Multi-peak soliton	$a_1 = 0.5, b_1 = 2$
Quasi-sine-wave	$a_1 = 0.5, b_1 = 5$
Quasi-periodic anti-dark soliton	$a_1 = 0.01, b_1 = 1.24$

Remark 2 Equation (1.8) is composed of hyperbolic and trigonometric functions, so the transformed waves are nonlinear superpositions of solitary and periodic waves.

Remark 3 $\beta_1(\theta_1 + \ln\sqrt{\lambda_2} = 0)$ and $\beta_2(\Lambda_1 = 0)$ are the characteristic lines of the transformed waves. The two characteristic lines are parallel, and the distance between them is a function of the time t. As the time changes, the geometry of the characteristic lines also changes, thus having the evolution of the other transformed waves.

Theorem 1.2 *The transformed wave solution $\widetilde{u}_2$ of the (2+1)-dimensional modified Boussinesq equation can be expressed as:*

$$
\begin{aligned}
\widetilde{u}_2 &= 2[\ln(2\sqrt{\lambda_2}\cosh(\theta_1 + \ln\sqrt{\lambda_2})) + \lambda_1\cos\Lambda_1]_{xx} \\
&= \frac{8a_1^2\lambda_2 - 2b_1^2\lambda_1^2 + 4(a_1^2 - b_1^2)\lambda_1\sqrt{\lambda_2}\cosh(\theta_2 + \ln\sqrt{\lambda_2})\cos(\Lambda_2)}{(2\sqrt{\lambda_2}\cosh(\theta_2 + \ln\lambda_2) + \lambda_1\cos(\Lambda_2))^2} \\
&\quad + \frac{8a_1b_1\lambda_1\sqrt{\lambda_2}\sinh(\theta_2 + \ln\sqrt{\lambda_2})\sin(\Lambda_2)}{(2\sqrt{\lambda_2}\cosh(\theta_2 + \ln\sqrt{\lambda_2}) + \lambda_1\cos(\Lambda_2))^2},
\end{aligned} \tag{1.9}
$$

where parameters a_1, b_1 are arbitrary constant, $\theta_1, \lambda_1, \lambda_2$ are defined in Eq. (3.14). The relationship between various types of transformed waves and parameters is shown in Table 2.

Remark 4 a_1 is always smaller than b_1, periodicity of transformed waves is stronger when a_1 is much smaller than b_1.

Remark 5 Equation (1.9) is composed of hyperbolic and trigonometric functions, so the transformed waves are nonlinear superpositions of solitary and periodic waves.

Remark 6 $\beta_1(\theta_1 + \ln\sqrt{\lambda_2} = 0)$ and $\beta_2(\Lambda_1 = 0)$ are the characteristic lines of the transformed wave. At the point the two characteristic lines are parallel, and the distance between these characteristic lines is a function of the time t. As the time changes, the geometry of the characteristic lines also changes, thus having the evolution of the other transformed waves.

1.2 Plan of Proof

In this paper, the state transformation of nonlinear equations is studied. In order to study this problem, we must first obtain the soliton solution of the equation, the breather solution. So the structure of this paper is as follows:

In Sect. 2, we derive single soliton solution and double soliton solution of the (2+1)-dimensional sine-Gordon equation, and we prove Theorem 1.1 in subsection 2.2 and 2.3 of this chapter.

In Sect. 3, N-soliton solution and breather solution of the (2+1) dimensional modified Boussinesq equation are derived. Then the state transition problem of the equation is studied by the characteristic line analysis, Theorem 1.2 is proved here.

In Sect. 4, we summarize the previous work.

In Sect. 5, we say the future recommendations.

2 Breather Transition and Its Mechanism of (2+1)-Dimensional Sine-Gordon Equation

The (2+1)-dimensional sine-Gordon equation is given in the previous section. In this chapter, we mainly learn about the characteristic line of its solution.

2.1 Soliton Solution of (2+1)-Dimensional Sine-Gordon Equation

Let f be expanded in series according to the parameter ε as:

$$f = 1 + f^{(1)}\varepsilon + f^{(2)}\varepsilon^2 + \cdots + f^{(n)}\varepsilon^n + \cdots \cdots \tag{2.1}$$

Then we substitute Eq. (2.1) into Eq. (1.2), and collect the coefficients of the same degree ε to obtain the following equation:

$$\varepsilon : f_{xx}^{(1)} + f_{yy}^{(1)} - f_{tt}^{(1)} = \frac{1}{2}(f^{(1)} - (f^{(1)})^*), \tag{2.2}$$

$$\varepsilon^2 : 2(f_{xx}^{(2)} + f_{yy}^{(2)} - f_{tt}^{(2)}) + (D_x^2 + D_y^2 - D_t^2)(f^{(1)} \cdot f^{(1)})$$
$$= \frac{1}{2}((f^{(1)})^2 - ((f^{(1)})^*)^2) + f^{(2)} - (f^{(2)})^*, \tag{2.3}$$

$$\varepsilon^3 : (f_{xx}^{(3)} + f_{yy}^{(3)} - f_{tt}^{(3)}) + (D_x^2 + D_y^2 - D_t^2)(f^{(1)} \cdot f^{(2)})$$
$$= \frac{1}{2}(f^{(3)} - (f^{(3)})^* + f^{(1)}f^{(2)} - (f^{(1)})^*(f^{(2)})^*). \tag{2.4}$$
$$\cdots \cdots$$

2.1.1 Single Soliton Solution

Since f is any complex function here, let's set

$$f^{(1)} = e^{\xi_1} \cdot e^{\frac{i\pi}{2}}, \xi_1 = k_1 x + l_1 y + w_1 t + \gamma_1, \tag{2.5}$$

where k_1, l_1, w_1, γ_1 are all real numbers, substituting Eq. (2.5) into Eq. (2.2), we get

$$k_1^2 + l_1^2 - w_1^2 = 1. \tag{2.6}$$

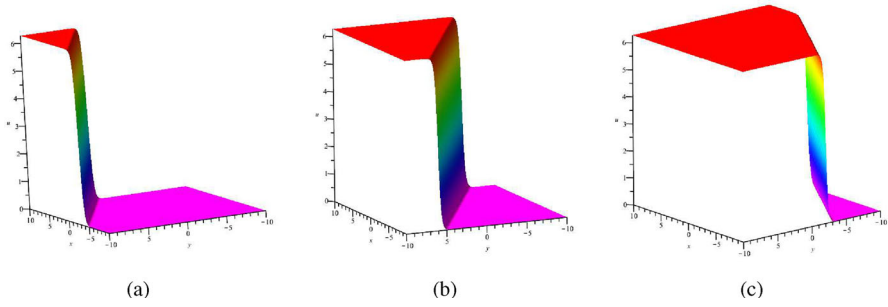(a)   (b)   (c)

Fig. 1 Structure of Single Soliton Solutions as t changes. **a** $t = -7$. **b** $t = 0$. **c** $t = 7$. Parameters $k_1 = 3, l_1 = 5, \gamma_1 = 0, w_1 = \sqrt{k_1^2 + l_1^2 - 1} = \sqrt{33}$

Then we substitute the Eq. (2.5) into (2.3),

$$f_{xx}^{(2)} + f_{yy}^{(2)} - f_{tt}^{(2)} = \frac{1}{2}(f^{(2)} - (f^{(2)})^*). \tag{2.7}$$

The same as Eq. (2.1), so let $f^{(2)} = 0$, we get

$$f_{xx}^{(3)} + f_{yy}^{(3)} - f_{tt}^{(3)} = \frac{1}{2}(f^{(3)} - (f^{(3)})^*). \tag{2.8}$$

Here we take $f^{(3)} = 0$, in turn, we can get $f^{(4)} = f^{(5)} = \cdots = 0$. So if we set $\varepsilon = 1$, then

$$f_1 = 1 + f^{(1)} = 1 + e^{\xi_1} \cdot e^{\frac{i\pi}{2}}. \tag{2.9}$$

By substituting the above equation into Eq. (1.5), we obtain the single soliton solution of this equation.

$$u_1 = 2i \ln \frac{f_1^*}{f_1} = 2i \ln \frac{1 - i e^{\xi_1}}{1 + i e^{\xi_1}} = 4 \arctan(e^{\xi_1}). \tag{2.10}$$

Thus, we can get the three-dimensional diagram of its soliton solution at time $t = -7, 0, 7$.

2.1.2 Double Soliton Solution

In order to find a double soliton solution to the equation, let's set

$$f^{(1)} = (e^{\xi_1} + e^{\xi_2}) \cdot e^{\frac{i\pi}{2}}, \xi_j = k_j x + l_j y + w_j t + \gamma_j, j = 1, 2, k_j^2 + l_j^2 - w_j^2 = 1. \tag{2.11}$$
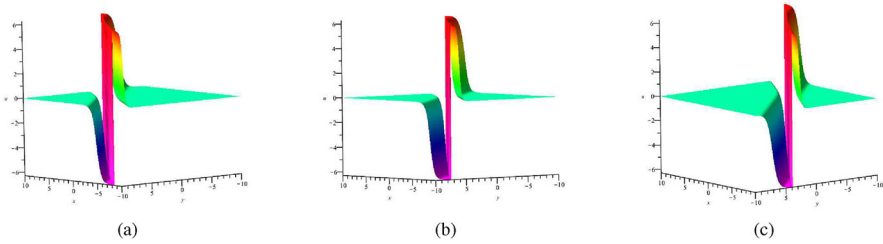
Fig. 2 Structure of Double Soliton Solutions as t changes. **a** $t = -1$. **b** $t = 0$. **c** $t = 1$. Parameters $k_1 = 3, l_1 = 5, k_2 = 2, l_2 = 2, \gamma_1 = \gamma_2 = 0, w_1 = \sqrt{k_1^2 + l_1^2 - 1} = \sqrt{33}, w_2 = \sqrt{k_2^2 + l_2^2 - 1} = \sqrt{7}$

By plugging in Eq. (2.3) and setting $f^{(2)} = e^{\xi_1 + \xi_2 + A_{12}} \cdot e^{i\pi}$, among them the first index of the last item for soliton interactions, so we can get

$$e^{A_{12}} = \frac{(k_1 - k_2)^2 + (l_1 - l_2)^2 - (w_1 - w_2)^2}{(k_1 + k_2)^2 + (l_1 + l_2)^2 - (w_1 + w_2)^2},$$

then

$$f_2 = 1 + f^{(1)} + f^{(2)} = 1 + (e^{\xi_1} + e^{\xi_2}) \cdot e^{\frac{i\pi}{2}} + e^{\xi_1 + \xi_2 + A_{12}} \cdot e^{i\pi}. \quad (2.12)$$

By substituting the above equation into (1.2), we derive the double soliton solution of the equation

$$u_2 = 2i \ln \left(\frac{f^*}{f} \right) = 4 \arctan \left(\frac{e^{\xi_1} + e^{\xi_2}}{1 - e^{\xi_1 + \xi_2 + A_{12}}} \right). \quad (2.13)$$

We use mathematical software again to draw a three-dimensional diagram of the double soliton solution at time $t = -1, 0, 1$ as shown in Fig. 2.

2.2 The Breather Solution and Characteristic Line Analysis of (2+1)-Dimensional Sine-Gordon Equation

In order to obtain the breather solution of the (2+1)-dimensional sine-Gordon equation, we pluralize the wave number of the double soliton solution u_2, i.e., Eq. (2.13). Let's set

$$k_1 = k_2^* = a_1 + ib_1, l_1 = l_2^* = p_1 + iq_1, \gamma_1 = \gamma_2^* = \ln \frac{\lambda_1}{2} + \delta_1 + \eta_1, \quad (2.14)$$

where $a_1, b_1, p_1, q_1, \lambda_1, \delta_1, \eta_1$ are real numbers, we plug in (2.12)

$$f_2 = 1 + e^{\frac{i\pi}{2}} (e^{\theta_1 + i\Lambda_1 + \ln \frac{\lambda_1}{2}} + e^{\theta_1 - i\Lambda_1 + \ln \frac{\lambda_1}{2}}) + e^{2\theta_1 + 2\ln \frac{\lambda_1}{2} + A_{12} + i\pi}$$

$$= 1 + \lambda_1 e^{\theta_1 + \frac{i\pi}{2}} \cos(\Lambda_1) + \frac{\lambda_1^2 H}{4} e^{2\theta_1 + i\pi}, \quad (2.15)$$

where

$$\theta_1 = a_1 x + p_1 y + \sqrt{\rho} \cos \frac{\alpha_1}{2} t + \delta_1,$$

$$\Lambda_1 = b_1 x + q_1 y + \sqrt{\rho} \sin \frac{\alpha_1}{2} t + \eta_1,$$

$$H = e^{A_{12}} = \frac{(k_1 - k_2)^2 + (l_1 - l_2)^2 - (w_1 - w_2)^2}{(k_1 + k_2)^2 + (l_1 + l_2)^2 - (w_1 + w_2)^2}$$

$$= \frac{-4b_1^2 - 4q_1^2 - ((a_1 + ib_1)^2 + (p_1 + iq_1)^2 - (a_1 - ib_1)^2 - (p_1 - iq_1)^2)^2}{4b_1^2 + 4q_1^2 - ((a_1 + ib_1)^2 + (p_1 + iq_1)^2 - 2 + (a_1 - ib_1)^2 + (p_1 - iq_1)^2)^2},$$

$$\rho \cos \alpha_1 = a_1^2 + p_1^2 - b_1^2 - q_1^2 - 1,$$

$$\rho \sin \alpha_1 = 2a_1 b_1 + 2p_1 q_1, \tag{2.16}$$

then we take

$$\lambda_2 = \frac{\lambda_1^2 H}{4} e^{i\pi}, \lambda_3 = \lambda_1 e^{\frac{i\pi}{2}}.$$

In order to better reflect the characteristics of breather, we will be on both sides of Eq. (2.15) at the same time divided by e^{θ_1}, the resulting

$$\frac{f_2}{e^{\theta_1}} = e^{-\theta_1} + \lambda_3 \cos(\Lambda_1) + \lambda_2 e^{\theta_1}$$

$$= 2\sqrt{\lambda_2} \frac{\sqrt{\lambda_2} e^{\theta_1} + \frac{e^{\theta_1}}{\sqrt{\lambda_2}}}{2} + \lambda_3 \cos(\Lambda_1)$$

$$= 2\sqrt{\lambda_2} \cosh(\theta_1 + \ln \sqrt{\lambda_2}) + \lambda_3 \cos(\Lambda_1).$$

Thus,

$$f_2 \sim 2\sqrt{\lambda_2} \cosh(\theta_1 + \ln \sqrt{\lambda_2}) + \lambda_3 \cos(\Lambda_1). \tag{2.17}$$

Therefore, we get its breather solution by substituting Eq. (2.17) into (1.5), i.e.,

$$u_2 = 2i \ln \left(\frac{f^*}{f} \right) = 2i \ln \left(\frac{(2\sqrt{\lambda_2} \cosh(\theta_1 + \ln \sqrt{\lambda_2}) + \lambda_3 \cos \Lambda_1)^*}{2\sqrt{\lambda_2} \cosh \theta_1 + \ln \sqrt{\lambda_2} + \lambda_3 \cos \Lambda_1} \right). \tag{2.18}$$

If f_2 is converted to Eq. (2.17), It can be seen that the breather solution u_2 is localized and periodic, where the hyperbolic function (cosh, sinh) determines its localization and the hyperbolic function (cos, sin) determines its periodicity. Therefore, the breather structure can be considered as a family of solitary wave and periodic wave components. In order to better understand the wave state of the breather, we need to analyze the characteristic lines of the solitary wave and the periodic wave. According to the derivation process, we get two characteristic lines $\beta_1(\theta_1 + \ln \sqrt{\lambda_2} = 0)$ and
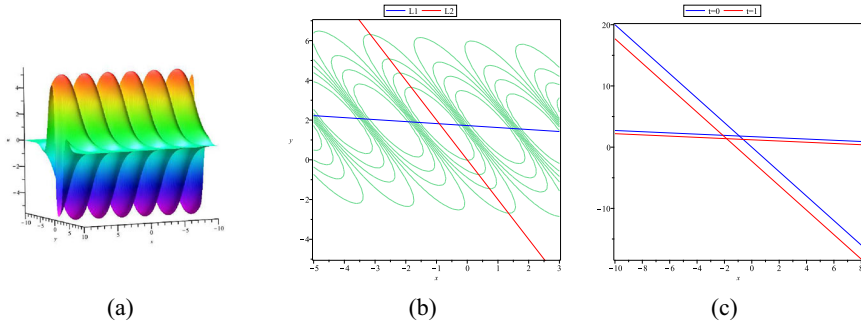
Fig. 3 **a** Spatial structure of the breather solution at $t = 0$. **b** The contour figure of **a**. L1 and L2 represent the characteristic lines. **c** The characteristic lines of **a** in the (x, y)-plane at $t = 0$ and $t = 1$. Parameters $a_1 = 0.1, b_1 = 2, p_1 = 1, q_1 = 1, \lambda_1 = 2, \delta_1 = 0, \eta_1 = 0$. $L1 = 0.1x + y + 0.5230469914t - 1.723950496$, $L2 = 2x + y + 2.294248931t$.

$\beta_2(\Lambda_1 = 0)$ of the breather. Notice that the solitary wave component is traveling at $\frac{\sqrt{\rho}\cos\frac{\alpha_1}{2}}{a_1}$ velocity on the x-axis, and $\frac{\sqrt{\rho}\cos\frac{\alpha_1}{2}}{p_1}$ on the y-axis. The propagation velocity of the periodic wave in the x-axis is $\frac{\sqrt{\rho}\cos\frac{\alpha_1}{2}}{b_1}$, and the propagation velocity in the y-axis is $\frac{\sqrt{\rho}\cos\frac{\alpha_1}{2}}{q_1}$.

Figure 3 is the three-dimensional diagram of breather at $t = 0$, the contour diagram and the characteristic diagram at $t = 0, 1$.

From Fig. 3, we can see that the angle between the two characteristic lines does not change with time. So we cannot help but ask under what conditions are the two feature lines parallel? What happens to its wave state in this case? This is what we are going to study next in the equation breather state transition problem.

2.3 State Transition of Breather in (2+1)-Dimensional Sine-Gordon Equation

Through the previous analysis, we know that the two characteristic lines of the breather are:

$$\beta_1 : a_1x + p_1y + \sqrt{\rho}\cos\frac{\alpha_1}{2}t + \delta_1 + \ln\sqrt{\lambda_2} = 0, \qquad (2.19)$$

$$\beta_2 : b_1x + q_1y + \sqrt{\rho}\cos\frac{\alpha_1}{2}t + \eta_1 = 0. \qquad (2.20)$$

Then the condition that the two characteristic lines are parallel is:

$$\begin{vmatrix} a_1 & p_1 \\ b_1 & q_1 \end{vmatrix} = 0.$$

Then we get a relation: $a_1q_1 - b_1p_1 = 0$, further we can know

$$\frac{b_1}{a_1} = \frac{q_1}{p_1} = l, \qquad (2.21)$$

where l is a constant, then we can analyze how the breather changes under the condition of parallel characteristic lines according to this relation, that is, how its wave state changes.

From (2.21), we can get $b_1 = la_1, q_1 = lp_1$. Then we obtain the breather solutions in the new form,

$$f_2 \sim 2\sqrt{\lambda_2} \cosh(\theta_1 + \ln \sqrt{\lambda_2}) + \lambda_3 \cos(\Lambda_1), \tag{2.22}$$

where

$$\theta_1 = a_1 x + p_1 y + \sqrt{\rho} \cos \frac{\alpha_1}{2} t + \delta_1,$$

$$\Lambda_1 = la_1 x + lp_1 y + \sqrt{\rho} \sin \frac{\alpha_1}{2} t + \eta_1,$$

$$H = e^{A_{12}} = \frac{(k_1 - k_2)^2 + (l_1 - l_2)^2 - (w_1 - w_2)^2}{(k_1 + k_2)^2 + (l_1 + l_2)^2 - (w_1 + w_2)^2}$$

$$= \frac{-4b_1^2 - 4q_1^2 - ((a_1 + ib_1)^2 + (p_1 + iq_1)^2 - (a_1 - ib_1)^2 - (p_1 - iq_1)^2)^2}{4b_1^2 + 4q_1^2 - ((a_1 + ib_1)^2 + (p_1 + iq_1)^2 - 2 + (a_1 - ib_1)^2 + (p_1 - iq_1)^2)^2}$$

$$= \frac{-4(la_1)^2 - 4(lp_1)^2 - ((a_1 + ila_1)^2 + (p_1 + ilq_1)^2 - (a_1 - ila_1)^2 - (p_1 - ilp_1)^2)^2}{4(la_1)^2 + 4(lp_1)^2 - ((a_1 + ila_1)^2 + (p_1 + ilp_1)^2 - 2 + (a_1 - ila_1)^2 + (p_1 - ilp_1)^2)^2},$$

$$\lambda_2 = \frac{\lambda_1^2 H}{4} e^{i\pi}, \quad \lambda_3 = \lambda_1 e^{\frac{i\pi}{2}}. \tag{2.23}$$

By substituting in (1.5), we get

$$\tilde{u}_2 = 2i \ln \frac{f_2^*}{f_2} = 2i \ln \left(\frac{(2\sqrt{\lambda_2} \cosh(\theta_1 + \ln \sqrt{\lambda_2}) + \lambda_3 \cos(\Lambda_1))^*}{2\sqrt{\lambda_2} \cosh(\theta_1 + \ln \sqrt{\lambda_2}) + \lambda_3 \cos(\Lambda_1)} \right). \tag{2.24}$$

From the perspective of form alone, Eq. (2.24) and (2.18) have no difference, but they are different in essence. The solitary wave and periodic wave of Eq. (2.24) solution are superimposed in the same direction, and the characteristic direction is the same, that is to say

$$\theta_2 = \kappa_1 \Lambda_2 + \kappa_2. \tag{2.25}$$

So we use the characteristic line expression to define the characteristic direction angle,

$$\varphi = \arctan \left(\frac{p_1}{a_1} \right),$$

where φ is the positive angle between the characteristic line and the y-axis, which needs to be distinguished from the general definition.

Since f is a complex function, so $\frac{f_2^*}{f}$ can be written in exponential form, then $\ln(\frac{f_2^*}{f})$ can be converted, then we have to consider the conditions required in the
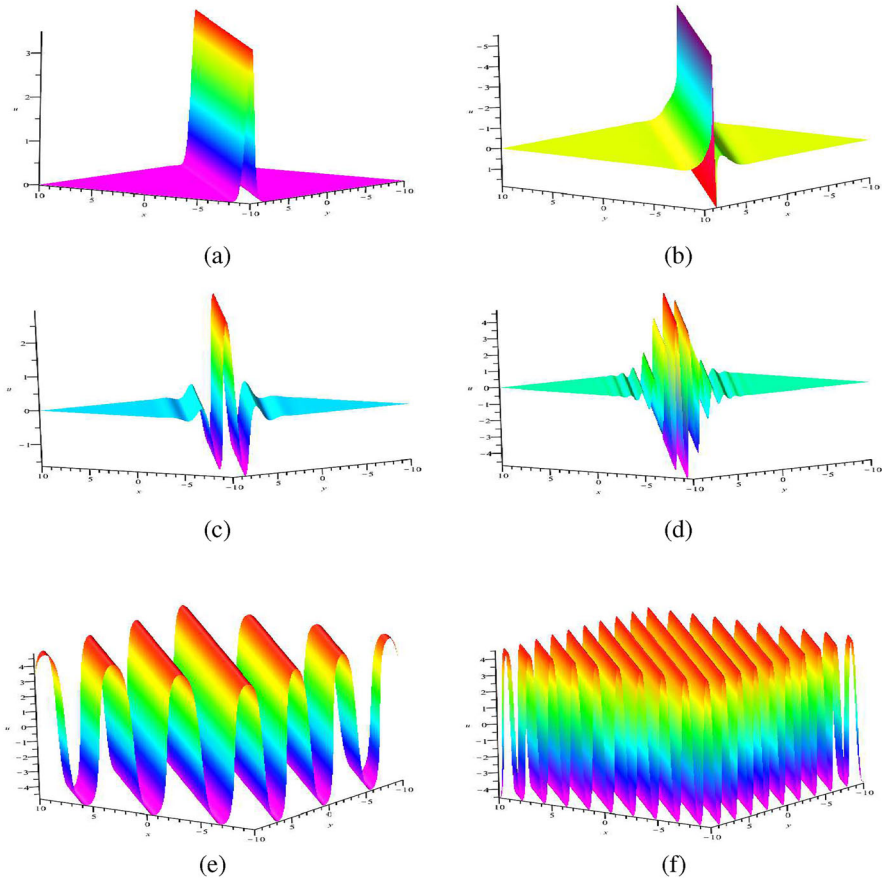
Fig. 4 Spatial structure of the transformed nonlinear wave solution at $t = 0$. **a** Quasi-anti-dark soliton. Parameters $l = \frac{1}{3}, a_1 = 3, b_1 = 1, p_1 = 3, q_1 = 1$. **b** M-type soliton. Parameters $l = 1, a_1 = 1, b_1 = 1, p_1 = 1, q_1 = 1$. **c** Oscillating M-type soliton. Parameters $l = 2, a_1 = 1, b_1 = 2, p_1 = 1, q_1 = 2$ **d** Multi-peak soliton. $l = 5, a_1 = 1, b_1 = 5, p_1 = 1, q_1 = 5$. **e** Quasi-sine-wave. Parameters $l = 1000, a_1 = 0.001, b_1 = 1, p_1 = 0.001, q_1 = 1$. **f** Quasi-periodic anti-dark soliton. Parameters $l = 3000, a_1 = 0.001, b_1 = 3, p_1 = 0.001, q_1 = 3, l = \frac{b_1}{a_1}$. Other parameters $\lambda_1 = 2, \delta_1 = 0, \eta_1 = 0$

function f, according to Eq. (2.22) we can know that $\lambda_2 \neq 0$, then $H \neq 0$. According to equation (2.21), the breather can be converted into other waves under the condition that the characteristic lines are parallel. Then we get three-dimensional maps of the other nonlinear waves by using mathematical software.

Figure 4 is based on the change of wave-number ratio l. In Fig. 4, it can be found that when $l = \frac{1}{3}$, the breather transforms into a quasi-anti-dark soliton with only one extreme line and is symmetric about the characteristic direction. When $l = 1$, the breather transforms into an M-type soliton with three extreme lines, one crest and two troughs. When $l = 2$, the breather again becomes an oscillating M-type soliton. When $l = 5$, the breather is transformed into multi-peak soliton, $l = 1000$, is transformed into quasi-sine wave, and $l = 3000$, is transformed into quasi-periodic anti-dark soliton.

In this case, there is almost no localization in other directions, and the localization of waves is almost only shown in the characteristic direction. It can be seen that with the increase of the parameter l, the transformation of the breather into other waves follows the following rules: quasi-anti-dark soliton → M-type soliton → oscillating M-type soliton → multi-peak soliton → quasi-sine wave → quasi-periodic anti-dark soliton.

From Fig. 4, we find that parameter condition $a_1 > b_1$ represents waves with strongly solitary states and weakly periodic states, while $a_1 < b_1$ represents waves with weakly solitary states and strongly periodic states. So when a_1 increase, nonlinear wave solitons sexual enhancement, b_1 increases, the nonlinear wave periodic enhancement. We can verify this conclusion with images.

Since the above results are obtained by fixing the time $t = 0$, what effect does the time change have on the transformed waves? Next, we continue to study the effect of time change on the transformed waves.

We can get from the previous work that the characteristic line of the transformed waves are:

$$\beta_3 : a_1 x + p_1 y + \sqrt{\rho} \cos \frac{\alpha_1}{2} t + \delta_1 + \ln \sqrt{\lambda_2} = 0, \tag{2.26}$$

$$\beta_4 : l a_1 x + l p_1 y + \sqrt{\rho} \cos \frac{\alpha_1}{2} t + \eta_1 = 0. \tag{2.27}$$

The direction of the two characteristic lines is the same, but the velocity is different. For its solitary wave component, its velocity on the x-axis and y-axis are respectively:

$$V_{1,x} = \frac{\sqrt{\rho} \cos \frac{\alpha_1}{2}}{a_1},$$

$$V_{1,y} = \frac{\sqrt{\rho} \cos \frac{\alpha_1}{2}}{p_1}.$$

For the periodic wave component, its velocity on the x-axis and y-axis are:

$$V_{2,x} = \frac{\sqrt{\rho} \cos \frac{\alpha_1}{2}}{l a_1},$$

$$V_{2,y} = \frac{\sqrt{\rho} \cos \frac{\alpha_1}{2}}{l p_1}.$$

So the two characteristic line with change with the change of time, set the distance of two characteristic line is d_1, we have

$$d_1 = \frac{\left| \left(\frac{\sqrt{\rho} \sin \frac{\alpha_1}{2}}{l} - \sqrt{\rho} \cos \frac{\alpha_1}{2} \right) t + \frac{\eta_1}{l} - \delta_1 - \ln \sqrt{\lambda_2} \right|}{\sqrt{a_1^2 + p_1^2}}.$$

It can be seen that with the change of time, the distance between the two characteristic lines also changes, and the shape of the transformed waves also changes.

The following is an analysis of the different transformed waves. The first is the quasi-anti-dark soliton at different times, whose three-dimensional maps are drawn by Maple software.
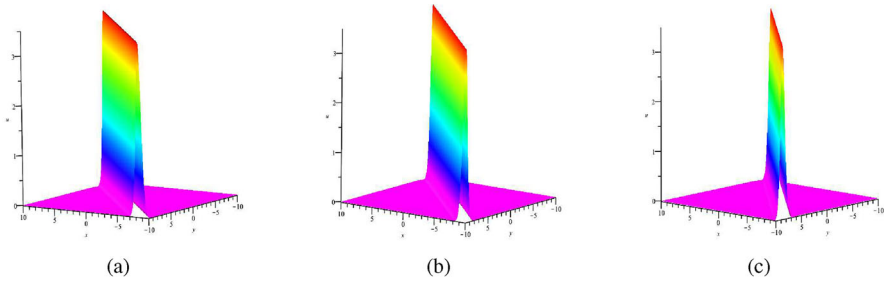
Fig. 5 Structure of the quasi-anti-dark soliton as t changes. **a** $t = -1$. **b** $t = 0$. **c** $t = 1$. Parameters $l = \frac{1}{3}, a_1 = 3, b_1 = 1, p_1 = 3, q_1 = 1, \lambda_1 = 2, \delta_1 = 0, \eta_1 = 0$
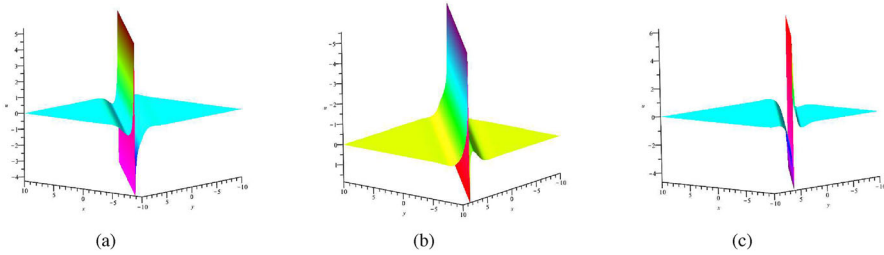

Fig. 6 Structure of M-type soliton as t changes. **a** $t = -1$. **b** $t = 0$. **c** $t = 1$. Parameters $l = 1, a_1 = 1, b_1 = 1, p_1 = 1, q_1 = 1, \lambda_1 = 2, \delta_1 = 0, \eta_1 = 0$

As shown in Fig. 5, the time change does not have much effect on quasi-anti-dark soliton.

Next is a three-dimensional diagram of M-type soliton at different times.

It is found from the Fig. 6 that time change has a great influence on M-type soliton.

3 Breather Transition and Its Mechanism of the (2+1)-Dimensional Modified Boussinesq Equation

This chapter we continue to study the N-soiton solution of the (2+1)-dimensional modified Boussinesq equation by using the Hirota bilinear method, and construct the breather solution by wave number pluralization, and study the state transition of the equation.

The (2+1)-dimensional modified Boussinesq equation to be studied in this chapter is given in the previous section.

3.1 Soliton Solution of the (2+1)-Dimensional Modified Boussinesq Equation

Based on the Hirota bilinear method, we get the N-soliton solution of Eq. (1.5):

$$u_N = 2(\ln f_N)_{xx}, \quad f_N = \sum_{\mu=0,1} \exp\left(\sum_{j=1}^{N} \mu_j \xi_j + \sum_{1 \leq j < l}^{N} \mu_j \mu_l A_{jl}\right), \quad (3.1)$$
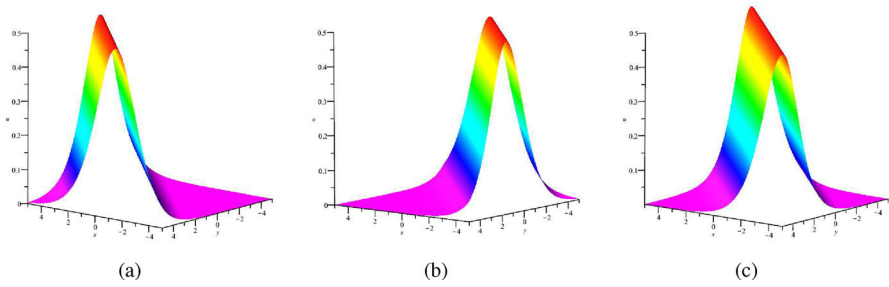
Fig. 7 Structure of Single Soliton Solutions as t changes. **a** $t = -2$. **b** $t = 0$. **c** $t = 2$. Parameters $k_1 = 1, p_1 = 1, w_1 = \sqrt{1 + k_1^2 + p_1^2} = \sqrt{3}, \gamma_1 = 0$

where

$$e^{A_{jl}} = -\frac{(k_j w_j - k_l w_l)^2 - (k_j - k_l)^2 - (k_j p_j - k_l p_l)^2 - (k_j - k_l)^4}{(k_j w_j + k_l w_l)^2 - (k_j + k_l)^2 - (k_j p_j + k_l p_l)^2 - (k_j + k_l)^4},$$

$$\xi_i = k_i(x + p_i y + w_i t) + \gamma_i, \ w_i^2 = 1 + k_i^2 + p_i^2, i = 1, 2.$$

3.1.1 Single Soliton Solution

When $N = 1$, we can get the single soliton solution of this equation:

$$u_1 = 2(\ln f_1)_{xx} = 2(\ln(1 + e^{\xi_1}))_{xx} = \frac{k_1^2}{2}\left(\text{sech}\,\frac{\xi_1}{2}\right)^2. \tag{3.2}$$

By using mathematical software, we can get the three-dimensional diagram of its soliton solution at time $t = -2, 0, 2$ as shown in Fig. 7.

3.1.2 Double Soliton Solution

f_2 is represented as follows:

$$f_2 = 1 + e^{\xi_1} + e^{\xi_2} + e^{\xi_1 + \xi_2 + A_{12}}, \tag{3.3}$$

where $e^{A_{12}} = -\frac{(k_1 w_1 - k_2 w_2)^2 - (k_1 - k_2)^2 - (k_1 p_1 - k_2 p_2)^2 - (k_1 - k_2)^4}{(k_1 w_1 + k_2 w_2)^2 - (k_1 + k_2)^2 - (k_1 p_1 + k_2 p_2)^2 - (k_1 + k_2)^4}$. So, we get the double soliton solution of the equation

$$u_2 = 2(\ln f_2)_{xx} = 2(\ln(1 + e^{\xi_1} + e^{\xi_2} + e^{\xi_1 + \xi_2 + A_{12}}))_{xx}. \tag{3.4}$$

We use mathematical software again to draw a three-dimensional diagram of the double soliton solution at time $t = -1, 0, 1$. As shown in Fig. 8.
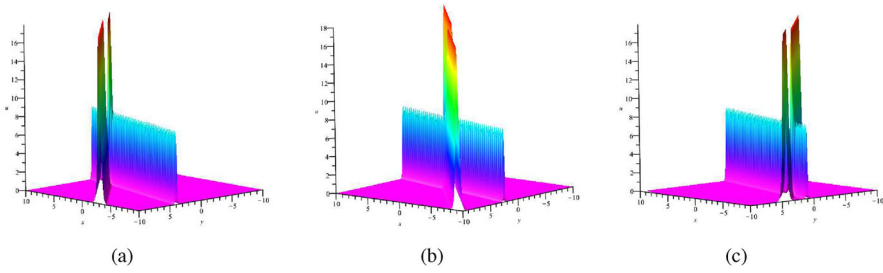
Fig. 8 Structure of Double Soliton Solutions as t changes. **a** $t = -1$. **b** $t = 0$. **c** $t = 1$. Parameters $k_1 = 6$, $p_1 = 1$, $k_2 = 4$, $p_2 = 4$, $\gamma_1 = \gamma_2 = 0$, $w_1 = \sqrt{k_1^2 + p + 1} = \sqrt{38}$, $w_2 = \sqrt{k_2^2 + p_2^2 + 1} = \sqrt{33}$

3.2 The Breather Solution and Characteristic Line Analysis of the (2+1)-Dimensional Modified Boussinesq Equation

We use the double soliton solution in Sect. 2 of this chapter to pluralize the wave number of Eq. (3.4). Let

$$k_1 = k_2^* = a_1 + ib_1, \, p_1 = p_2^* = c_1 + id_1, \, \gamma_1 = \gamma_2^* = \ln \frac{\lambda_1}{2} + \delta_1 + i\eta_1, \quad (3.5)$$

where $a_1, b_1, c_1, d_1, \lambda_1, \delta_1, \eta_1$ are real numbers, we plug in (3.3),

$$
\begin{aligned}
f_2 &= 1 + e^{\theta_1 + i\Lambda_1 + \ln \frac{\lambda_1}{2}} + e^{\theta_1 - i\Lambda_1 + \ln \frac{\lambda_1}{2}} + e^{2\theta_1 + 2\ln \frac{\lambda_1}{2} + A_{12}} \\
&= 1 + \lambda_1 e^{\theta_1} \cos(\Lambda_1) + \frac{\lambda_1^2 H}{4} e^{2\theta_1},
\end{aligned}
\quad (3.6)
$$

where

$$\theta_1 = a_1 x + (a_1 c_1 - b_1 d_1)y + \sqrt{\rho}(a_1 \cos \frac{\alpha_1}{2} - b_1 \sin \frac{\alpha_1}{2})t + \delta_1,$$

$$\Lambda_1 = b_1 x + (a_1 d_1 + b_1 c_1)y + \sqrt{\rho}(a_1 \sin \frac{\alpha_1}{2} + b_1 \cos \frac{\alpha_1}{2})t + \eta_1,$$

$$H = e^{A_{12}} = -\frac{(k_1 w_1 - k_2 w_2)^2 - (k_1 - k_2)^2 - (k_1 p_1 - k_2 p_2)^2 - (k_1 - k_2)^4}{(k_1 w_1 + k_2 w_2)^2 - (k_1 + k_2)^2 - (k_1 p_1 + k_2 p_2)^2 - (k_1 + k_2)^4},$$

$$\rho \cos \alpha_1 = a_1^2 + c_1^2 - b_1^2 - d_1^2 + 1,$$

$$\rho \sin \alpha_1 = 2a_1 b_1 + 2c_1 d_1. \quad (3.7)$$

Let's set

$$\lambda_2 = \frac{\lambda_1^2 H}{4}.$$

In order to better reflect the characteristics of the breather, we will be on both sides of Eq. (3.6) at the same time divided by e^{θ_1}, the resulting is

$$\frac{f_2}{e^{\theta_1}} = e^{-\theta_1} + \lambda_1 \cos(\Lambda_1) + \lambda_2 e^{\theta_1}$$

$$= 2\sqrt{\lambda_2} \frac{\sqrt{\lambda_2} e^{\theta_1} + \frac{e^{\theta_1}}{\sqrt{\lambda_2}}}{2} + \lambda_1 \cos(\Lambda_1)$$

$$= 2\sqrt{\lambda_2} \cosh(\theta_1 + \ln\sqrt{\lambda_2}) + \lambda_1 \cos(\Lambda_1),$$

thus,

$$f_2 \sim 2\sqrt{\lambda_2} \cosh(\theta_1 + \ln\sqrt{\lambda_2}) + \lambda_1 \cos(\Lambda_1). \tag{3.8}$$

Then we get its breather solution by substituting the equation (3.8) into (1.6).

$$u_2 = 2(\ln f_2)_{xx} = 2[\ln 2\sqrt{\lambda_2} \cosh(\theta_1 + \ln\sqrt{\lambda_2}) + \lambda_1 \cos\Lambda_1]_{xx}$$

$$= \frac{8a_1^2\lambda_2 - 2b_1^2\lambda_1^2 + 4(a_1^2 - b_1^2)\lambda_1\sqrt{\lambda_2}\cosh(\theta_1 + \ln\sqrt{\lambda_2})\cos(\Lambda_1)}{2\sqrt{\lambda_2}\cosh(\theta_1 + \ln\sqrt{\lambda_2}) + \lambda_1\cos(\Lambda_1))^2} \tag{3.9}$$

$$+ \frac{8a_1 b_1 \lambda_1 \sqrt{\lambda_2} \sinh(\theta_1 + \ln\sqrt{\lambda_2}) \sin\Lambda_1}{(2\sqrt{\lambda_2}\cosh(\theta_1 + \ln\sqrt{\lambda_2}) + \lambda_1\cos(\Lambda_1))^2}.$$

As a result of $f_2 > 0$, and $2\cosh(\theta_1 + \ln\sqrt{\lambda_2}) + \lambda_1 \cos(\Lambda_1))$ has the minimum value of $2\sqrt{\lambda_2} - |\lambda_1|$, so when $\lambda_2 > \frac{\lambda_1^2}{4}$, i.e.$H > 1$, there is a non-singular solution to Eq. (3.9).

If f_2 is converted to Eq. (3.8), it can be seen that the breather solution u_2 is local and periodic, in which the hyperbolic function (cosh, sinh) determines its locality, and the hyperbolic function (cos, sin) determines its periodicity. This kind of breather is a combination of the two components of solitary wave and periodic wave. In order to better understand the wave state of the breather, we need to analyze the characteristic lines of the solitary wave component and the periodic wave component. According to the derivation process, we get two characteristic lines $\beta_1(\theta_1 + \ln\sqrt{\lambda_2} = 0)$ and $\beta_2(\Lambda_1 = 0)$ of the breather.

We can see from the characteristic lines that the propagation velocity of the solitary wave in the x-axis is $\frac{\sqrt{\rho}(a_1 \cos\frac{\alpha_1}{2} - b_1 \sin\frac{\alpha_1}{2})}{a_1}$ and in the y-axis is $\frac{\sqrt{\rho}(a_1 \cos\frac{\alpha_1}{2} - b_1 \sin\frac{\alpha_1}{2})}{a_1 c_1 - b_1 d_1}$. the periodic wave component is traveling at $\frac{a_1 \sin\frac{\alpha_1}{2} + b_1 \cos\frac{\alpha_1}{2}}{b_1}$ velocity on the x-axis, and $\frac{a_1 \sin\frac{\alpha_1}{2} + b_1 \cos\frac{\alpha_1}{2}}{a_1 d_1 + b_1 c_1}$ on the y-axis. Observing the expression of the characteristic lines, we can see that the angle (or parallel) between the two characteristic lines does not change with time, from a physical point of view, which shows that the shape and amplitude of the breather do not change with time, only the phase changes with time.

Figure 9 is the three-dimensional diagram of breather at $t = 0$,the contour diagram and the characteristic diagram at $t = 0, 1$.
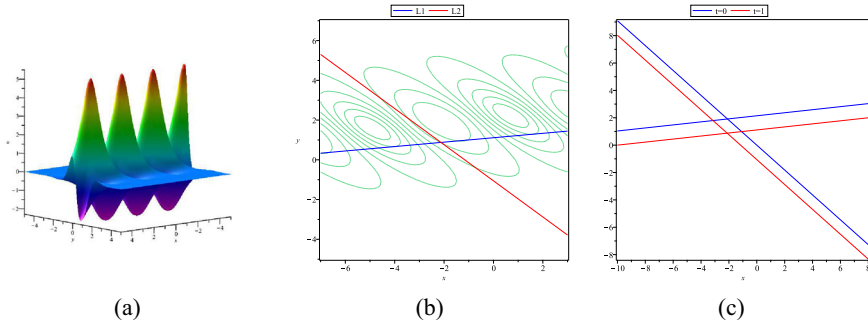
Fig. 9 **a** Spatial structure of the breather solution at $t = 0$. **b** The contour figure of **a**. $L1$ and $L2$ represent the characteristic lines. **c** The characteristic lines of **a** in the (x, y)-plane at $t = 0$ and $t = 1$. Parameters $a_1 = 0.1$, $b_1 = 1$, $c_1 = 1$, $d_1 = 1$, $\lambda_1 = 2$, $\delta_1 = \eta_1 = 0$. $L1 = 0.1x - 0.9y - 0.9311534897t + 1.931492390$, $L2 = x + 1.1y + 1.164034421t$

As shown in Fig. 9, under the above parameters, two characteristic lines intersect and the angle does not change with time, then we will also have a question, under what conditions will two characteristic lines be parallel? What happens to the breather in this case? If it changes, will it change in the same way as in the previous chapter? This is the state transition problem of this nonlinear wave that we want to study.

3.3 State Transition of Breather for (2+1)-Dimensional Modified Boussinesq Equation

Through the previous analysis, we know that the two characteristic lines of breather are:

$$\beta_1 : a_1 x + (a_1 c_1 - b_1 d_1) y + \sqrt{\rho} \left(a_1 \cos \frac{\alpha_1}{2} - b_1 \sin \frac{\alpha_1}{2} \right) t + \delta_1 + \ln \sqrt{\lambda_2} = 0,$$

$$(3.10)$$

$$\beta_2 : b_1 x + (a_1 d_1 + b_1 c_1) y + \sqrt{\rho} \left(a_1 \cos \frac{\alpha_1}{2} - b_1 \sin \frac{\alpha_1}{2} \right) t + \eta_1 = 0. \qquad (3.11)$$

Then the condition that the two characteristic lines are parallel is that the following determinant is zero.

$$\begin{vmatrix} a_1 & a_1 c_1 - b_1 d_1 \\ b_1 & a_1 d_1 + b_1 c_1 \end{vmatrix} = 0.$$

Then we get a relation: $(a_1^2 - b_1^2)d_1 = 0$, so when $a_1^2 - b_1^2 \neq 0$, $d_1 = 0$, so at this time

$$H = \frac{\sqrt{-b_1^2 - 2ia_1 b_1 + a_1^2 + c_1^2 + 1} \cdot \sqrt{-b_1^2 + 2ia_1 b_1 + a_1^2 + c_1^2 + 1} - a_1^2 + 7b_1^2 - c_1^2 - 1}{\sqrt{-b_1^2 - 2ia_1 b_1 + a_1^2 + c_1^2 + 1} \cdot \sqrt{-b_1^2 + 2ia_1 b_1 + a_1^2 + c_1^2 + 1} - 7a_1^2 + b_1^2 - c_1^2 - 1}.$$

$$(3.12)$$

When $a_1 = 0.5, b_1 = 2, c_1 = 1, H = 9.77$, this satisfies nonsingular conditions, and in this case the characteristic lines are parallel. All the transformed waves in the following paper satisfy the non-singular condition.

Next we'll let $d_1 = 0$ in breather solutions in the equation of a new form:

$$f_2 \sim 2\sqrt{\lambda_2} \cosh(\theta_1 + \ln\sqrt{\lambda_2}) + \lambda_1 \cos(\Lambda_2), \qquad (3.13)$$

where

$$\theta_2 = a_1 x + a_1 c_1 y + \sqrt{\rho}(a_1 \cos\frac{\alpha_1}{2} - b_1 \sin\frac{\alpha_1}{2})t + \delta_1,$$

$$\Lambda_2 = b_1 x + b_1 c_1 y + \sqrt{\rho}(a_1 \sin\frac{\alpha_1}{2} + b_1 \cos\frac{\alpha_1}{2})t + \eta_1,$$

$$H = \frac{\sqrt{-b_1^2 - 2ia_1b_1 + a_1^2 + c_1^2 + 1} \cdot \sqrt{-b_1^2 + 2ia_1b_1 + a_1^2 + c_1^2 + 1} - a_1^2 + 7b_1^2 - c_1^2 - 1}{\sqrt{-b_1^2 - 2ia_1b_1 + a_1^2 + c_1^2 + 1} \cdot \sqrt{-b_1^2 + 2ia_1b_1 + a_1^2 + c_1^2 + 1} - 7a_1^2 + b_1^2 - c_1^2 - 1},$$

$$\lambda_2 = \frac{\lambda_1^2 H}{4}. \qquad (3.14)$$

By substituting in (3.4), we get

$$\begin{aligned}
\tilde{u}_2 = 2(\ln f_2)_{xx} &= 2[\ln(2\sqrt{\lambda_2}\cosh(\theta_1 + \ln\sqrt{\lambda_2})) + \lambda_1 \cos\Lambda_1]_{xx} \\
&= \frac{8a_1^2\lambda_2 - 2b_1^2\lambda_1^2 + 4(a_1^2 - b_1^2)\lambda_1\sqrt{\lambda_2}\cosh(\theta_2 + \ln\sqrt{\lambda_2})\cos(\Lambda_2)}{(2\sqrt{\lambda_2}\cosh(\theta_2 + \ln\lambda_2) + \lambda_1\cos(\Lambda_2))^2} \\
&\quad + \frac{8a_1 b_1 \lambda_1 \sqrt{\lambda_2}\sinh(\theta_2 + \ln\sqrt{\lambda_2})\sin(\Lambda_2)}{(2\sqrt{\lambda_2}\cosh(\theta_2 + \ln\sqrt{\lambda_2}) + \lambda_1\cos(\Lambda_2))^2}. \qquad (3.15)
\end{aligned}$$

From the perspective of form alone, Eqs. (3.15) and (3.9) have no difference, but they are different in essence. The solitary wave and periodic wave of Eq. (3.15) solution are superimposed in the same direction, and the characteristic direction is the same, that is to say,

$$\theta_2 = \kappa_1 \Lambda_2 + \kappa_2. \qquad (3.16)$$

So we use the characteristic line expression to define the characteristic direction angle,

$$\varphi = \arctan c_1,$$

where φ is the positive angle between the characteristic line and the y-axis, which needs to be distinguished from the general definition.

In other words, when we fixed c_1, under the condition of characteristic line parallel of the characteristics of nonlinear wave direction does not change, and when $H > 1$, the equation has a non-singular solution, then the breather can be converted into various other types of waves, such as quasi-antidark solitons, M-type solitons, oscillating M-type solitons, multimodal solitons, quasi-sine waves, and quasi-periodic waves.
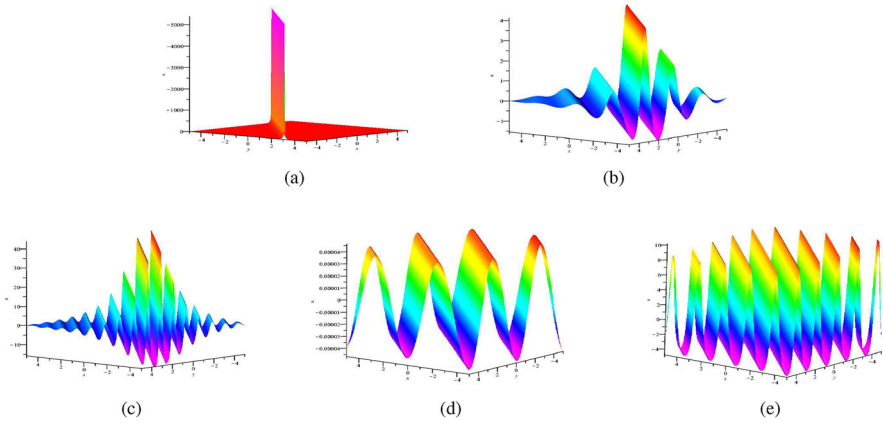
Fig. 10 Spatial structure of the transformed nonlinear wave solution at $t = 0$. **a** Quasi-anti-dark soliton. Parameters $l = 2, a_1 = 1, b_1 = 2$ **b** Oscillating M-type soliton. Parameters $l = 2, a_1 = 0.5, b_1 = 2$ **c** Multi-peak soliton. $l = 10, a_1 = 0.5, b_1 = 5$ **d** Quasi-sine wave. Parameters $l = 124, a_1 = 0.01, b_1 = 1.24$ **e** Quasi-periodic anti-dark soliton. Parameters $l = 300, a_1 = 0.01, b_1 = 3.l = \frac{b_1}{a_1}$. Other parameters $c_1 = 1, \lambda_1 = 2, \delta_1 = 0, \eta_1 = 0$

Figure 10 is a 3D diagram of the conversion of the breather into other types of waves under different conditions at $t = 0$ time.

Same as the analysis in the previous chapter, we can find that the transformed waves also change with the change of the wave-number ratio $l = \frac{b_1}{a_1}$. When the wave-number ratio increases, the transformed waves change as follows: quasi-anti-dark soliton $\rightarrow$ oscillating M-type soliton $\rightarrow$ multi-peak soliton $\rightarrow$ quasi-sine wave $\rightarrow$ quasi-periodic anti-dark soliton.

At the same time we find in the process a_1 is always smaller than b_1, and when the a_1 is far less than b_1, periodicity of the transformed waves is stronger.

Since the above results are obtained by fixing the time $t = 0$, what effect does the time change have on the transformed waves? Next, we continue to study the effect of time change on transformed waves.

We know from the previous work that the characteristic line of the conversion wave is:

$$\beta_3 : a_1 x + a_1 c_1 y + \sqrt{\rho} \left(a_1 \cos \frac{\alpha_1}{2} - b_1 \sin \frac{\alpha_1}{2} \right) t + \delta_1 + \ln \sqrt{\lambda_2} = 0, \quad (3.17)$$

$$\beta_4 : b_1 x + b_1 c_1 y + \sqrt{\rho} \left(a_1 \sin \frac{\alpha_1}{2} + b_1 \cos \frac{\alpha_1}{2} \right) t + \eta_1 = 0. \quad (3.18)$$

The direction of the two characteristic lines is the same, but the propagation velocity is different. For its solitary wave component, its propagation velocity on the x-axis and y-axis are respectively:

$$V_{1,x} = \frac{\sqrt{\rho}(a_1 \cos \frac{\alpha_1}{2} - b_1 \sin \frac{\alpha_1}{2})}{a_1},$$
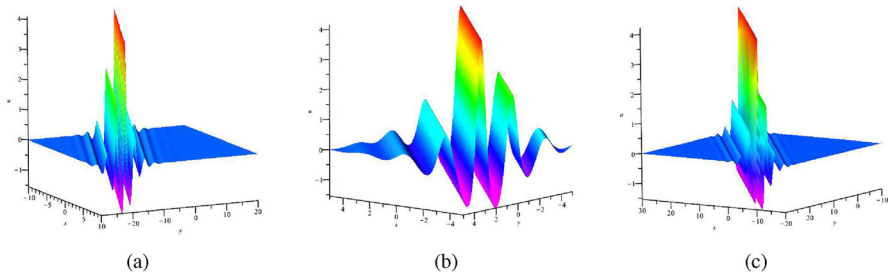
Fig. 11 Structure of the oscillating M-type soliton as t changes. **a** $t = -2$. **b** $t = 0$. **c** $t = 4$. Parameters $l = 4, a_1 = 0.5, b_1 = 2, c_1 = 1, \lambda_1 = 2, \delta_1 = 0, \eta_1 = 0$

$$V_{1,y} = \frac{\sqrt{\rho}(a_1 \cos \frac{\alpha_1}{2} - b_1 \sin \frac{\alpha_1}{2})}{a_1 c_1}.$$

For the periodic wave component, its propagation velocity on the x-axis and y-axis are:

$$V_{2,x} = \frac{\sqrt{\rho}(a_1 \sin \frac{\alpha_1}{2} + b_1 \cos \frac{\alpha_1}{2})}{b_1},$$

$$V_{2,y} = \frac{\sqrt{\rho}(a_1 \sin \frac{\alpha_1}{2} + b_1 \cos \frac{\alpha_1}{2})}{b_1 c_1}.$$

So the two characteristic line with change with the change of time, set the distance of two characteristic line is d_2, then

$$d_2 = \frac{|\frac{a_1^2 + b_1^2}{a_1 b_1} \sqrt{\rho} \sin \frac{\alpha_1}{2} t + \frac{\eta_1}{b_1} - \frac{\delta_1}{a_1} - \frac{\ln \sqrt{\lambda_2}}{a_1}|}{\sqrt{1 + c_1^2}}.$$

It can be seen that with the change of time, the distance between the two characteristic lines also changes, and the shape of the transformed waves also changes.

The following is an analysis of the different transformed waves. Since we have analyzed quasi-antidark solitons in the previous chapter, we would hazard a guess that time change has no effect on it, and we can verify this conclusion by plotting. So next we study the oscillating M-type solitons, the following is the change of the transformed wave at different times.

The following Fig. 11 shows the oscillating M-type soliton at $t = -2, 0, 4$.

Through observation, we can find that the change of time has a certain effect on the transformed waves such as oscillating M-type soliton.

4 Conclusions

In this paper, bilinear forms of two (2+1)-dimensional equations are studied and their breather solutions are obtained, and we derive the state transition problem by using their breather solutions. The results are as follows:

1. We get the soliton solution and breather solution of the (2+1)-dimensional Sine-Goedon equation via Hirota bilinear method, and derive the conversion conditions of the breather into other waves. We also analyze the influence of wave number ratio on solitary wave and periodic wave, and learn obout the influence of time change on transformed waves.

2. Similarly, we use the same method to obtain N-soliton solution of the (2+1)-dimensional modified Boussinesq equation, and then obtain its breather solution by wave number pluralization. And when the two characteristic lines are parallel, that is to say, $H > 1$, the breather can be converted into other types of nonlinear waves. In addition, we find that the difference in wave-number ratio also affects the solitary and periodic waves.

3. Through the analysis of the above two equations, we find that both breathers and transformed waves are formed by the nonlinear superposition of solitary waves and periodic waves, the difference is the characteristic direction of the solitary waves and periodic waves, and the conversion conditions of the breather into other waves of the two equations are different, but the difference in wave number ratio has an impact on both solitary waves and periodic waves. And the change of time also has an effect on some transformed waves.

Through the analysis in this paper, we can know that the breathers and other non-linear waves are formed by the nonlinear superposition of solitary waves and periodic waves. In addition, we try to investigate the dynamics process of nonlinear transformed waves over time. And from the perspective of the change of the geometric structure of the characteristic lines, the principle behind it is analyzed. In the future work, we will focus on studying the conversion mechanisms of higher-dimensional equations, including not only the problem of converting the states of the equation breather, but also the conversion mechanism of the equation lump wave, and so on. This work will be beneficial for the study of nonlinear physics, fluid dynamics, solitons, and other related fields.

5 Future Recommendations

The (2+1)-dimensional sine-Gordon equation has significant applications in studying the motion of charged particles in nonlinear fields, field coupling in quantum field theory, and other related problems. The (2+1)-dimensional modified Boussinesq equation is a widely applicable tool for describing the propagation of nonlinear waves in various fields of study, including water wave theory. They are particularly useful for describing phenomena such as ocean waves, optical waves, and fluctuations in solid materials. Therefore, in the future we can explore more analytical and numerical solutions of these two equations to deepen our understanding of them. Further mechanisms of nonlinear wave transitions can also be investigated and attempts can be made to apply these mechanisms to other nonlinear dynamical systems to explore their generalisability and application. We can also extend the research results to other fields, such as biomedical engineering and seismology, to explore the significance and potential applications of breather conversion in different fields.

Author Contributions The authors read and approved the final manuscript.

Data Availability Data sharing not applicable to this article as no datasets were generated or analyzed during the current study.

Declarations

Conflict of interest The author declares that they have no Conflict of interest.

References

1. Lamb, G.L.: Elements of soliton theory. Adv. Math. **32**(7), 215 (1981)
2. Camassa, R., Hyman, J.M., Luce, B.P.: Nonlinear waves and solitons in physical systems. Phys. D **123**, 1–20 (1998)
3. Ahmad, J., Akram, S., Noor, K., Nadeem, M., Bucur, A., Alsayaad, Y.: Soliton solutions of fractional extended nonlinear Schrödinger equation arising in plasma physics and nonlinear optical fiber. Sci. Rep. **13**(1), 10877 (2023)
4. Gao, X.Y.: Oceanic shallow-water investigations on a generalized Whitham-Broer-Kaup-Boussinesq-Kupershmidt system. Phys. Fluids **35**, 127106 (2023)
5. Gao, X.Y., Guo, Y.J., Shan, W.R.: Ultra-short optical pulses in a birefringent fiber via a generalized coupled Hirota system with the singular manifold and symbolic computation. Appl. Math. Lett. **140**, 108546 (2023)
6. Gao, X.Y.: Letter to the Editor on the Korteweg-de Vries-type systems inspired by Results Phys. 51, 106624 (2023) and 50, 106566 (2023). Results Phys. **53**, 106932 (2023)
7. Gao, X.Y.: Considering the wave processes in oceanography, acoustics and hydrodynamics by means of an extended coupled (2+1)-dimensional Burgers system. Chin. J. Phys. **86**, 572–577 (2023)
8. Gao, X.Y.: Two-layer-liquid and lattice considerations through a (3+1)-dimensional generalized Yu-Toda-Sasa- Fukuyama system. Appl. Math. Lett. **152**, 109018 (2024)
9. Gao, X.T., Tian, B.: Water-wave studies on a (2+1)-dimensional generalized variable-coefficient Boiti-Leon-Pempinelli system. Appl. Math. Lett. **128**, 107858 (2022)
10. Russell, J.S.: Report on waves. Report of fourteenth meeting of British Association for the Advancement of Science, pp.311–390. John Murray, York, London (1844)
11. Korteweg, D.J., Vries, G.D.: On the change of form of long waves advancing in a rectangular canal, and on a new type of long stationary waves. Lond. Edinb. Dublin Philos. Mag. J. Sci. **39**(240), 422–433 (1895)
12. Zabusky, N.J., Kruskal, M.D.: Interaction of "Solitons" in a Collisionless Plasma and the Recurrence of Initial States. Phys. Rev. Lett. **15**(6), 33–34 (1965)
13. Rehman, H.U., Said, G.S., Amer, A., Ashraf, H., et al.: Unraveling the (4+1)-dimensional Davey-Stewartson-Kadomtsev-Petviashvili equation: exploring soliton solutions via multiple techniques. Alex. Eng. J **90**, 17–23 (2024)
14. Dey, P.S., Lamiaa, H., Tharwat, M.M., Sarker, S., et al.: Soliton solutions to generalized (3+1)-dimensional shallow water-like equation using the $(\phi'/\phi, 1/\phi)$-expansion method. Arab. J. Basic Appl. Sci **31**(1), 121–131 (2024)
15. Dhosseini, K., Alizadeh, F., Sadri, K., et al.: Lie vector fields, conservation laws, bifurcation analysis, and Jacobi elliptic solutions to the Zakharov-Kuznetsov modified equal-width equation. Opt. Quantum Electron. **56**(4), 506 (2024)
16. Rasid, M.M., Miah, M.M., Ganie, A.H., et al.: Further advanced investigation of the complex Hirota-dynamical model to extract soliton solutions. Mod. Phys. Lett. B **38**(10), 2450074 (2024)

17. Malik, S., Hashemi, M.S., Kumar, S., et al.: Application of new Kudryashov method to various nonlinear partial differential equations. Opt. Quantum Electron. **55**(1), 8 (2023)
18. Raza, N., Osman, M.S., Abdel-Aty, A.H.: Optical solitons of space-time fractional Fokas-Lenells equation with two versatile integration architectures. Adv. Differ. Equ. **2020**, 157 (2020)
19. Akbar, M.A., Wazwaz, A.M., Mahmud, F., et al.: Dynamical behavior of solitons of the perturbed nonlinear Schrödinger equation and microtubules through the generalized Kudryashov scheme. Results Phys. **43**, 106079 (2022)
20. Chen, Y.Q., Tang, Y.H., Manafian, J., et al.: Dark wave, rogue wave and perturbation solutions of Ivancevic option pricing model. Nonlinear Dyn. **105**, 2539–2548 (2021)
21. Fahim, M.R.A., Kundu, P.R., Islam, M.E., et al.: Wave profile analysis of a couple of (3+1)-dimensional nonlinear evolution equations by sine-Gordon expansion approach. J. Ocean. Eng. Sci. **7**(3), 272–279 (2022)
22. Kumar, D., Park, C., Tamanna, N., Paul, G.C., Osman, M.S.: Dynamics of two-mode Sawada-Kotera equation: mathematical and graphical analysis of its dual-wave solutions. Results Phys. **19**, 103581 (2020)
23. Ablowitz, M.A., Clarkson, P.A.: Solitons, Nonlinear Evolution Equations and Inverse Scattering, vol. 3, pp. 2301–2305. Cambridge University Press, Cambridge (1991)
24. Zhou, T.Y., Tian, B., Shen, Y., Gao, X.T.: Auto-Bäcklund transformations and soliton solutions on the nonzero background for a (3+1)-dimensional Korteweg-de Vries-Calogero-Bogoyavlenskii-Schif equation in a fluid. Nonlinear Dyn. **111**(9), 8647–8658 (2023)
25. Celledoni, E., Marthinsen, H., Owren, B.: An introduction to Lie group integrators − basics, new developments and applications. J. Comput. Phys. **257**, 1040–1061 (2014)
26. Wu, X.H., Gao, Y.T.: Generalized Darboux transformation and solitons for the Ablowitz-Ladik equation in an electrical lattice. Appl. Math. Lett. **137**, 108476 (2023)
27. Hietarinta, J.: Hirota's Bilinear Method and its Generalization. Int. J. Mod. Phys. A **12**(01), 43–51 (1997)
28. Lin, Z., Wen, X.Y.: Hodograph transformation, various exact solutions and dynamical analysis for the complex Wadati-Konno-Ichikawa-II equation. Phys. D **451**, 133770 (2023)
29. Hirota, R.: The Direct Method in Soliton Theory. Cambridge University Press, Cambridge (2004)
30. Ma, Y.L., Wazwaz, A.M., Li, B.Q.: Soliton resonances, soliton molecules, soliton oscillations and heterotypic solitons for the nonlinear Maccari system. Nonlinear Dyn. **111**(19), 18331–18344 (2023)
31. Ma, Y.L., Li, B.Q.: Phase transitions of lump wave solutions for a (2+1)-dimensional coupled Maccari system. Eur. Phys. J. Plus **139**(1), 93 (2024)
32. Ma, Y.L., Wazwaz, A.M., Li, B.Q.: Phase transition from soliton to breather, soliton-breather molecules, breather molecules of the Caudrey-Dodd-Gibbon equation. Phys. Lett. A **488**, 129132 (2023)
33. Ma, Y.L., Li, B.Q.: Soliton interactions, soliton bifurcations and molecules, breather molecules, breather-to-soliton transitions, and conservation laws for a nonlinear (3+1)-dimensional shallow water wave equation. Nonlinear Dyn. **112**(4), 2851–2867 (2024)
34. Li, B.Q., Ma, Y.L.: Breather, soliton molecules, soliton fusions and fissions, and lump wave of the Caudrey-Dodd-Gibbon equation. Phys. Scripta **98**(9), 095214 (2023)
35. Li, B.Q., Ma, Y.L.: Hybrid soliton and breather waves, solution molecules and breather molecules of a (3+1)-dimensional Geng equation in shallow water waves. Phys. Lett. A **463**, 128672 (2023)
36. Hasegawa, A., Tappert, F.: Transmission of stationary nonlinear optical pulses in dispersive dielectric fibers. II. Normal dispersion. Appl. Phys. Lett. **23**(4), 171–172 (1973)
37. Kivshar, Y.S.: Nonlinear dynamics near the zero-dispersion point in optical fibers. Phys. Rev. Lett. **43**(3), 1677 (1991)
38. Li, Z., Li, L., Tian, H.: New types of solitary wave solutions for the higher order nonlinear Schrödinger equation. Phys. Rev. Lett. **84**(18), 4096 (2000)
39. Liu, C., Yang, Z.Y., Zhao, L.C., et al.: State transition induced by higher-order effects and background frequency. Phys. Rev. E **91**(2), 022904 (2015)
40. Shen, Y., Tian, B., Zhou, T.Y., Cheng, C.D.: Multi-pole solitons in an inhomogeneous multi-component nonlinear optical medium. Chaos Solitons Fract. **171**, 113497 (2023)
41. Lin, Z., Wen, X.Y.: Singular-loop rogue wave and mixed interaction solutions with location control parameters for Wadati-Konno-Ichikawa equation. Nonlinear Dyn. **111**(4), 3633–3651 (2023)
42. Dai, C.Q., Zhu, H.P.: Superposed Akhmediev breather of the (3+1)-dimensional generalized nonlinear Schrödinger equation with external potentials. Ann. Phys. **341**, 142–152 (2014)

43. Li, Z.D., Wu, X., Li, Q.Y., He, P.B.: Kuznetsov-Ma soliton and Akhmediev breather of higher-order nonlinear Schrödinger equation. Chin. Phys. B **25**(1), 10507–010507 (2016)
44. Hermann, A.H., William, S.W.: Solitons in optical communications. Rev. Mod. Phys. **68**(2), 423–444 (1996)
45. An, H.L., Feng, D., Zhu, H.X.: General M-lump, high-order breather and localized interaction solutions to the 2+1-dimensional Sawada-Kotera equation. Nonlinear Dyn. **87**(2), 1275–1286 (2019)
46. Jiang, L., Li, B.: Higher-order smooth positons and breather positons of sine-Gordon equation. Commun. Theor. Phys. **74**(8), 085006 (2022)
47. Ryabov, P.N.: Exact solutions of the Kudryashov-Sinelshchikov equation. Appl. Math. Comput **217**(7), 3585–3590 (2010)
48. Wu, J.J., Sun, Y.J., Li, B.: Degenerate lump chain solutions of (4+1)-dimensional Fokas equation. Results Phys. **45**, 106243 (2023)
49. Yang, S.X., Li, B.: ∂^--dressing method for the (2+1)-dimensional Korteweg-de Vries equation. Appl. Math. Lett. **140**, 108589 (2023)
50. Ma, W.X.: Lump solutions to the Kadomtsev-Petviashvili equation. Phys. Lett. A **379**(36), 1975–1978 (2015)
51. Pang, Y.M.: State transition of (2+1) dimensional Sawada-Kotera equation wave. Adv. Appl. Math. **10**(5), 7 (2021)
52. Yin, Z.Y., Tian, S.F.: Nonlinear wave transitions and their mechanisms of (2+1)-dimensional Sawada-Kotera equation. Phys. D **427**, 133002 (2021)
53. Chowdury, A., Ankiewicz, A., Akhmediev, N.: Moving breathers and breather-to-soliton conversions for the Hirota equation. Proc. R. Soc. A-Math. Phys. **471**(2180), 20150130 (2015)
54. Liu, C., Yang, Z.Y., Zhao, L.C., Yang, W.L.: State transition induced by higher-order effects and background frequency. Phys. Rev. E **91**(2), 022904 (2015)
55. Wang, L., Zhang, J.H., Wang, Z.Q., et al.: Breather-to-soliton transitions, nonlinear wave interactions, and modulational instability in a higher-order generalized nonlinear Schrödinger equation. Phys. Rev. E **93**(1), 012214 (2016)
56. Wang, C.J., Fang, H., Tang, X.X.: State transition of lump-type waves for the (2+1)-dimensional generalized KdV equation. Nonlinear Dyn. **95**, 2943–2961 (2019)
57. Rubinstein, J.: Sine-Gordon Equation. J. Math. Phys. **11**(1), 258–266 (1970)
58. Zhong, W.Y., Zhong, W.P., Milivoj, R.B., Cai, G.F.: Localized dynamical behavior in the (2+1)-dimensional sine-Gordon equation. Optik **204**, 164115 (2020)
59. Li, L.X., Su, T.: N-soliton Solution for a (2+1)-dimensional Modified Boussinesq Equation. Acta Math. Sci. **87**(04), 757–759 (2007)
60. Li, Z.T.: New kink-shaped solutions and periodic wave solutions for the (2+1)-dimensional sine-Gordon equation. Appl. Math. Comput. **215**(11), 3777–3781 (2010)
61. Martinov, N.K., Vitanov, N.K.: New class of running-wave solutions of the (2+1)-dimensional sine-Gordon equation. J. Phys. A **7**(13), 4611 (1994)
62. Charlier, C., Lenells, J.: Boussinesq's equation for water waves: asymptotics in sector V (2023) arXiv:2301.10669
63. McKean, H.P.: Boussinesq's equation on the circle. Commun. Pure Appl. Math. **34**(5), 599–691 (1981)
64. Moleleki, L.D., Khalique, C.M.: Solutions and conservation laws of a (2+1)-dimensional Boussinesq equation. Abstr. Appl. Anal. **2013**, 117–120 (2013)
65. Elsayed, S.M., Kaya, D.: The decomposition method for solving (2+1)-dimensional Boussinesq equation and (3+1)-dimensional KP equation. Appl. Math. Comput. **157**(2), 523–534 (2004)
66. Ma, C.H., Deng, A.P.: Lump Solution of (2+1)-dimensional Boussinesq equation. Commun. Theor. Phys. **65**(5), 546 (2016)